University of Groningen

High-Performance Smooth-Walled Horn Antennas for THz Frequency Range

Montofre, Daniel Arturo; Molina, Rocio; Khudchenko, Andrey; Hesper, Ronald; Baryshev, Andrey M.; Reyes, Nicolas; Mena, Fausto Patricio

IMPORTANT NOTE: You are advised to consult the publisher's version (publisher's PDF) if you wish to cite from it. Please check the document version below.

Document Version
Publisher's PDF, also known as Version of record

Publication date:
2019

[Link to publication in University of Groningen/UMCG research database](#)

High-Performance Smooth-Walled Horn Antennas for THz Frequency Range: Design and Evaluation

Daniel Arturo Montofré ⬤, Rocio Molina ⬤, Andrey Khudchenko ⬤, Ronald Hesper ⬤, Andrey M. Baryshev, Nicolas Reyes, and Fausto Patricio Mena ⬤

Abstract—Traditionally, corrugated conical horn antennas have been the main choice for use in astronomical receivers in the range of millimeter and submillimeter waves. They present low cross-polar level and high coupling efficiency into the fundamental Gaussian mode. However, this type of antenna is difficult to manufacture, inevitably increasing its price and extending the production process. In this article, we present two kinds of feed horn antennas, aimed for use in a frequency range equivalent to atacama large millimeter/submillimeter array (ALMA) Band 6 (211–275 GHz), which can be fabricated in a much simpler way with the conventional machining tools. Specifically, we present the design and performance comparison of smooth-walled spline-profile horns in two geometries, diagonal, and conical. Optimization of the designs has been made by means of an algorithm that allowed us to obtain models whose electrical and mechanical characteristics make them competitive when compared with corrugated horns. In particular, they are 40% shorter than the conventional corrugated horns suited for this band, representing an advantage given the stringent space constraints of most astronomical receivers. We also demonstrate that they can be coupled efficiently to an astronomical-grade optical system, using ALMA Band-6 receiver as an example. Furthermore, we have constructed the diagonal horn and characterized it thoroughly. Experimental results of the radiation pattern at room temperature show a good cross-polar performance with levels below −20 dB and Gaussicity above 96%. Our calculations show a good antenna-efficiency level with losses less than 1%. All these properties demonstrate the feasibility of this type of horns to become the main option at the time of choosing a feed system for cutting-edge astronomical applications.

D. A. Montofré is with the Department of Electrical Engineering, Universidad de Chile, Santiago 8370451, Chile, and also with the Kapteyn Institute of Astronomy, University of Groningen, 9747 AD Groningen, The Netherlands (e-mail: d.a.montofre@rug.nl).

R. Molina is with the Millimeter Wave Laboratory and the Department of Astronomy, Universidad de Chile, Santiago 7591245, Chile (e-mail: rocio.molina@raig.uchile.cl).

A. Khudchenko, R. Hesper, and A. M. Baryshev are with the Kapteyn Astronomical Institute, University of Groningen, 9747 AD Groningen, The Netherlands (e-mail: a.khudchenko@sron.nl; r.hesper@astro.rug.nl; a.m.baryshev@astro.rug.nl).

N. Reyes is with the Department of Electrical Engineering, Universidad de Chile, Santiago 8370451, Chile, and also with the Max-Planck Institute for Radio Astronomy, 53121 Bonn, Germany (e-mail: nireyes@uchile.cl).

F. P. Mena is with the Millimeter Wave Laboratory and the Department of Electrical Engineering, Universidad de Chile, Santiago 7591245, Chile (e-mail: fpmena@uchile.cl).

Color versions of one or more of the figures in this article are available online at http://ieeexplore.ieee.org.

Digital Object Identifier 10.1109/TTHZ.2019.2938985

I. INTRODUCTION

CORRUGATED conical horn antennas have been, traditionally, the main choice when it comes to developing instruments for astronomy applications in the range of millimeter and submillimeter waves (including part of the terahertz (THz) frequency spectrum) [1]. They have been selected due to their excellent characteristics. In particular, their coupling to the fundamental Gaussian mode (in short *Gaussicity*) is around 98% and a cross-polar level lower than −30 dB [2]. Nonetheless, this sort of antennas are difficult to manufacture, inevitably extending the production process, and therefore, increasing their price. There are other options to corrugated horns, e.g., conical and pyramidal horns. However, they lack symmetry in the radiation pattern, and additionally, pyramidal horns present astigmatism [3].

The diagonal horn was first described in 1962 [4], and subsequently, Johansson *et al.* [5] studied the feasibility to construct it using the split-block technique. They concluded that in this way integration to focal plane array could be easily implemented, with a negligible beam distortion. However, having a coupling to fundamental Gaussian mode of around 84% and a cross-polar level of around −15 dB, they are not the best option for astronomical applications. In 2002, Granet *et al.* [6] introduced the so-called smooth-walled spline-profile horn, as part of an upgrade program of The Australian Telescope [7]. They demonstrated that this horn achieved a performance in W-band that, in certain cases, has a competitive performance compared to its corrugated counterpart. Albeit the machining process was easier than the process to fabricate a corrugated horn, this is still somewhat complicated given the large numbers of steps taken to give the cubic spline shape to the walls. In 2018, Gibson *et al.* [8] took one step further combining the smooth-walled spline-profile horn with the ease of fabrication of the diagonal horn. The outcome was a new type of horn, designed for THz frequencies, easier to construct, and with a Gaussicity around 97% and a cross-polar level better than −20 dB. These features make this horn a good candidate to replace the corrugated horn in THz astronomical applications.

All these efforts reflect the increasing interest in replacing the corrugated horns with alternatives that have good performance
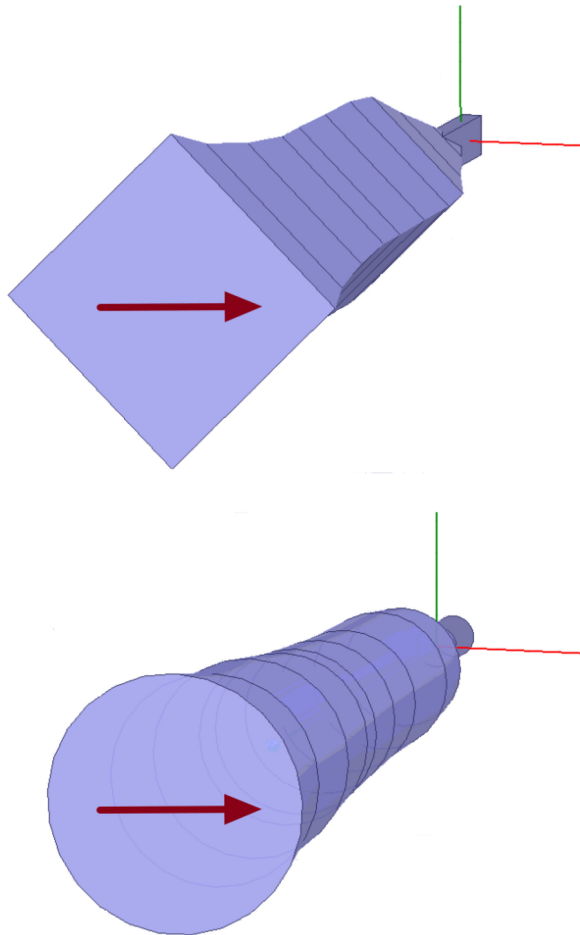
Fig. 1. Two horns under study. (Top) Diagonal-spline horn connected to a rectangular waveguide. (Bottom) Conical horn connected to a circular waveguide. Electric field orientation in input waveguide of the designs is represented by the brown arrow. It has been located at the aperture just to simplify its visualization. Both designs were optimized in order to reach the goals described in Table I.
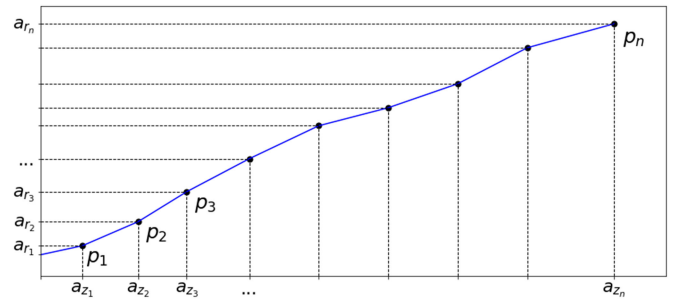

Fig. 2. Basic one-dimensional (1-D) profile of the smoothed-wall horn antennas. The shape of the horn wall is defined by the set of straight blue lines that connect each node (black dots labeled as p_i).

make the horns suitable for astronomical applications, and at the same time, keeping their construction easy and at low cost.

Our work demonstrates that a simplified profile can achieve similar or better performance when compared with other smooth-walled profiles [6], [8]. Simulations show good return losses with no necessity of flaring the input waveguide. Moreover, measurements show an improvement in various figures of merit. The beam has a more circular beam shape, cross-polar performance has levels lower than -20 dB, sidelobes are below -25 dB in the E and H cardinal planes, and the calculated Gaussicity exceeds 96%. Furthermore, we show that the smooth-walled horns studied here can be coupled efficiently to astronomical-grade receivers. As an example, we have calculated the coupling to the existing cold optical system of the ALMA Band 6.

II. DESIGN AND OPTIMIZATION

The starting point to design both horn antennas is the profile of the walls, which defines the features of the radiation pattern. We have followed a similar methodology as described in [16], i.e., define the wall shape using a spline curve and splitting that curve into several segments. Each of these segments are defined by two nodes (labeled as p_i), as shown in Fig. 2. In order to simplify the machining even further, we have used straight lines to connect nodes instead of a cubic spline curve. Each node is defined by a pair of coordinates (labeled as a_r and a_z), which are used as parameters for the optimization process. We selected a set of nine nodes to describe each horn, as a compromise between achieving the required goals and the use of computational resources. To define the initial position of the nodes, we started from a conventional diagonal, with the appropriate aperture, designed to operate in the desired frequency range. Then, we divided the straight profile into nine equal segments, which defines the initial position of the nodes.

Once the initial wall shape is defined, the next step is creating the volume. On the one hand, for the diagonal-spline horn, the volume is created by rotating the one-dimensional (1-D) wall profile in $90°$ and $-90°$, then each node is linked to its adjacent neighbors using straight lines. The result is a set of flat rectangular surfaces connecting the nodes that defines half of the volume of the horn. Then, the final volume is obtained by mirroring the resulting surface, by means of selecting the

(even at the expenses of some tradeoff), allow reproducibility, are easier to machine, and have an affordable cost. Not only astronomy but also other applications would benefit of such antennas since all of them are aiming to construct receivers at ever higher frequencies, and if possible, in the form of focal plane arrays [9]–[12]. In this article, we present the comparison of two types of smooth-walled spline-profile horn antennas, diagonal and circular (see Fig. 1), and the construction and characterization of one of them. This article has been focused on the frequency range covered by the atacama large millimeter/submillimeter array (ALMA) Band 6 (211–275 GHz), currently one of the most interesting observation bands for astronomers, with the image of HL-Tau [13] and the first image ever taken of a black hole event horizon [14] as examples of its major achievements. Nevertheless, the methodology described here is applicable to any kind of smoothed-wall horn antenna, no matter the applications nor the operating frequency range. This is particularly interesting because this method is scalable for higher frequencies, where the construction of corrugated horns is extremely difficult due to increasingly shorter wavelengths [15]. Our goal here is to

Target Function	Optimization Goal
Cross-polar	−20 dB
Sidelobes	−30 dB
S_{11}	−25 dB
Beam waist	∼2.0 mm

TABLE II
PROFILE PARAMETERS THAT DEFINE THE WALL
SHAPE FOR EACH HORN DESIGN

	Diagonal-Spline		Conical-Spline	
Parameter	a_z(mm)	a_r(mm)	a_z(mm)	a_r(mm)
p_1	2.50	0.73	3.90	1.88
p_2	5.50	1.55	6.50	2.18
p_3	8.10	2.35	10.40	2.25
p_4	10.10	2.54	13.50	2.45
p_5	12.40	2.56	16.30	2.63
p_6	14.80	2.61	17.70	2.75
p_7	19.50	2.93	21.50	3.19
p_8	23.30	3.51	25.70	3.41
p_9	27.50	4.25	30.30	4.17

proper symmetry axis. On the other hand, the conical spline is created by applying a $360°$ rotational sweep to the initial 1-D wall profile. Both horn geometries are shown in Fig. 1. The diagonal-spline and conical-spline horn designs are fed using a rectangular (0.5×1.0 mm) and a circular ($\varnothing 1.30$ mm) waveguide, respectively. This election was made to facilitate the subsequent machining process.

The optimization process for both horns was done using an HFSS [17] model, which takes the coordinates of each node as parameters. To make the horns suitable for astronomical applications, we have set the specifications listed in Table I as goals for the optimization. The goal of 2.0 mm for the beam waist was set as a reasonable value that could permit connecting the horn to an optical system. The optimization process starts from an initial set of points a_r and a_z. Then, these values are moved around their initial ones over certain range until the optimizer finds the set of points that better match the design specifications. This process was done for three key analysis frequencies, 211, 243, and 275 GHz (lowest, middle, and highest frequencies of the ALMA Band 6, respectively). The final set of parameters for each horn that better match the design specifications are listed in Table II. The aperture and length of each horn are defined by the coordinates of the node p_9. We can see that both designs have a similar dimension for their aperture, but the conical spline is 2.8 mm (or 9.24%) longer. Considering that the current corrugated horn of the Band-6 receiver has a length of 50.0 mm [18], the designs presented here are around 40% shorter. This is a big advantage taking into account the space restrictions presented in mostly all astronomical receivers.

III. PERFORMANCE EVALUATION OF DESIGNS

A. Analysis of Far-Field Beam Pattern Simulations

Fig. 3 shows the simulated far-field radiation pattern of the diagonal and conical spline horns at their three key analysis frequencies. Both horns show very good symmetry, above −20 dB,
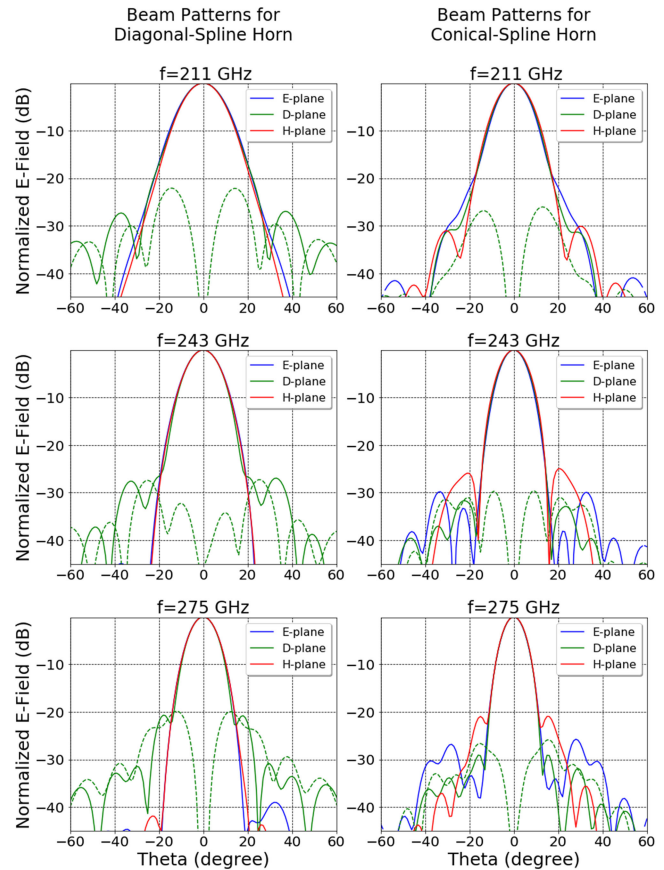

Fig. 3. Comparison of far-field radiation pattern for diagonal-spline (left column) and conical-spline horns at their key analysis frequencies. Copolar curves are shown in solid line, and cross-polar curves for the D plane are shown in dashed line. Diagonal-spline horn has lower level of sidelobes in E and H planes and a wider beam width. On the other hand, conical-spline horn exhibits lower sidelobes in the D plane, which correlates with lower levels of cross polar for all the frequencies.

for the E, D, and H planes. This means that both horns will produce a beam with good circular shape, or equivalently, they present low beam ellipticity.

The cross-polar levels for both designs are lower than −20 dB over the entire bandwidth. However, the conical-spline design shows a better performance at all frequencies, reaching levels close to −30 dB. This better cross-polar performance correlates with lower levels of sidelobes in the D plane. For the diagonal-spline geometry, the sidelobe level is below −40 dB in the E and H planes. The D plane shows higher levels of sidelobes with values above −30 dB for 211 and 243 GHz, and a level slightly below −20 dB for 275 GHz. For the conical-spline geometry, on the other hand, the sidelobe level is around −30 dB in the E, D, and H planes for 211 and 243 GHz. A difference is observed at 275 GHz, where the sidelobe level is slightly below −20 dB in the H plane. This difference in sidelobe level at different cardinal planes results in the diagonal-spline design having a more symmetrical beam shape, but at expenses of having higher levels of cross-polar component.

One additional issue to sort out at the moment of designing these antennas was the relatively wide bandwidth that must be
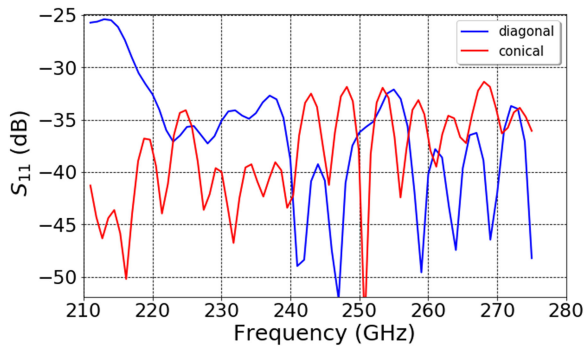
Fig. 4. Simulated return loss for diagonal-spline and conical-spline horns. Both designs show return loss levels below -25 dB for the entire frequency range.

TABLE III
CALCULATED PARAMETERS OF THE DIAGONAL-SPLINE HORN

Frequency (GHz)	w_o (mm)	θ_o (°)	PCL (mm)	Gain (dB)	Gaussicity %
211	2.00	12.9	4.34	21.6	97.0
243	2.02	11.1	3.23	23.5	97.2
275	2.10	9.4	0.61	25.0	96.9

TABLE IV
CALCULATED PARAMETERS OF THE CONICAL-SPLINE HORN

Frequency (GHz)	w_o (mm)	θ_o (°)	PCL (mm)	Gain (dB)	Gaussicity %
211	2.28	11.3	4.51	23.4	97.2
243	2.39	9.4	2.69	25.1	97.0
275	2.63	7.5	2.33	26.5	96.9

covered. These horns have a fractional bandwidth of 26.3%. A natural degradation can be seen as we move away from the central design frequency (243 GHz). Return losses (see Fig. 4) show a degradation only for the diagonal-spline design. However, this is below -25 dB, making the performance of return loss sufficiently good.

From the simulated far-field radiation patterns, we have calculated the beam waist (w_o), far-field divergence angle (θ_o), phase center location (PCL), gain, and Gaussicity [19]. The results are presented in Tables III and IV. The beam waist for the diagonal design is close to 2.0 mm at 211 and 243 GHz, but it shows a small deviation of 0.1 mm from the desired value at 275 GHz. In comparison, the beam waist of the conical design shows a larger deviation from the optimization goal. This difference in the beam waist correlates with the differences observed in the far-field divergence angle between designs. The calculated PCL (whose values indicate a position inside the horn, taking as reference plane the horn aperture) has a similar value at 211 GHz for both designs, but a significant difference is observed as the frequency increases. The impact of all these differences will be evaluated in next section, where as an example, the horns are coupled to the cold optical system of the ALMA Band-6 receiver. The calculated gain is within a range of 21–27 dB, which is expected for the traditional diagonal and conical horn. The values of Gaussicity were obtained by calculating the coupling integral, as described in [1], between the far-field radiation patterns and
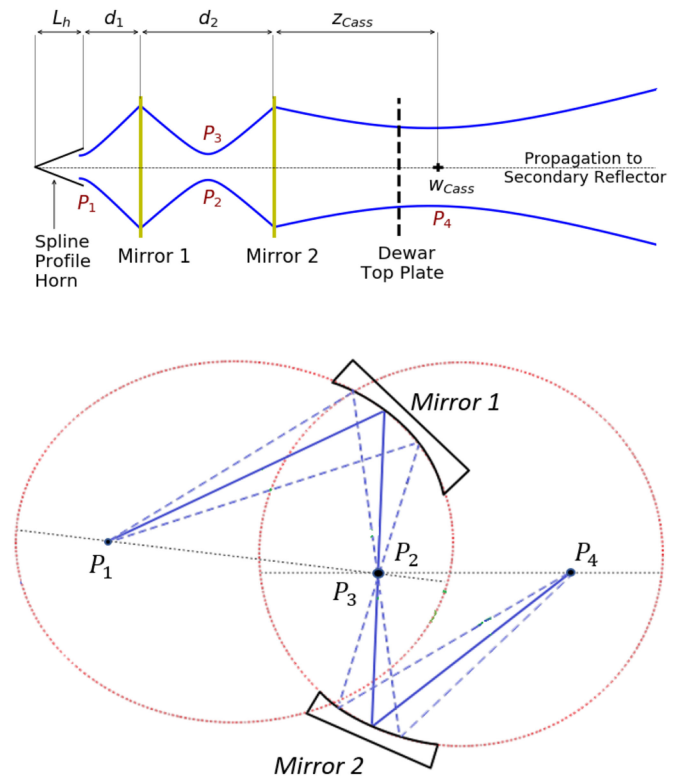

Fig. 5. (Top) Optical train description of the ALMA Band-6 optics, which consists of two elliptical mirrors (represented by yellow lines), and the spline-profile horn. The final beam waist and its position respect to mirror 2 are given by w_{cass} and z_{cass}, respectively. (Bottom) Mirror layout of ALMA Band-6 cold optical system. The points P_1 and P_2 represent the position of focal points for the mirror 1; P_3 and P_4 have the same relation with the mirror 2. The chief ray is shown by solid blue line.

their respective Gaussian fit curves. These values are close to 97% at the three key analysis frequency, which make these horns comparable with high performance corrugated horns, whose Gaussicity is in the order of 98% [20].

B. Example of Application: Integration into ALMA Band-6 Receiver

Although the horns presented here can be used as feed antennas in any astronomical system working around 243 GHz, as specific example, we have studied their integration with the cold optics of the current ALMA Band 6 for illuminating a secondary reflector with the same ALMA Cassegrain configuration. Quasi-optical calculations using the ABCD matrix formalism [21] have been performed to estimate the antenna efficiency when the designed diagonal- or conical-spline horn is coupled to the cold optical system. Fig. 5 shows the optical train description of the system under study and details of the system of elliptical mirrors used to match the horn beam into the secondary reflector [22]. The distance between the horn aperture and mirror 1 is represented as d_1, whereas d_2 represents the distance between mirrors 1 and 2. The focal points of elliptical mirrors (labeled as P_1, P_2, P_3, and P_4) have been chosen for optimal matching. The distance between the center of an elliptical mirror and one of its focal points P_i is denoted by R_i. Table V gives the optical

TABLE V
OPTICAL TRAIN PARAMETERS FOR EXISTING BAND-6 RECEIVERS

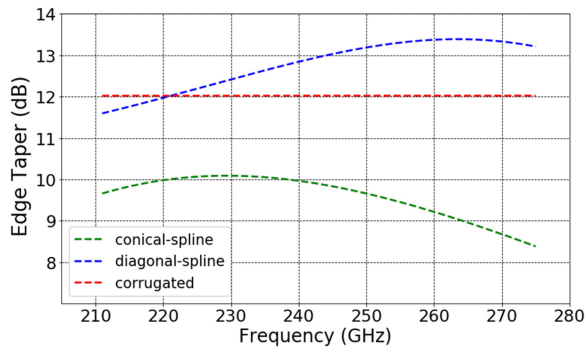| Optical-train parameter	Value (mm)
L_h	50.00
d_1	60.85
R_1	65.27
R_2	72.91
d_2	140.0
R_3	73.42
R_4	275.39

Fig. 6. Edge taper versus frequency when the Band-6 optical system is fed by different horns antennas.

train parameters that described the cold optical system of the existing ALMA Band-6 receiver [18].

Optimal illumination, i.e., maximum antenna efficiency, is achieved when the edge taper takes a value of around 12.02 dB, given the ALMA Cassegrain configuration [18]. The edge taper has been calculated, according to [19], as

$$T_e = 8.686 \left(\frac{r_s}{w_z} \right)^2$$

where r_s corresponds to the ALMA secondary reflector ($r_s = 375$ mm) and w_z is the beam radius at the secondary reflector position. The ALMA Band-6 corrugated horn was designed to have an edge taper of 12.02 dB over the entire frequency range [18]. This can be achieved if the beam waist and phase center location have constant values for all the frequencies. Fig. 6 shows the calculated edge taper as a function of frequency for the conical-spline, diagonal-spline, and corrugated horns. The edge taper have values ranging between 8.38 and 9.66 dB for the conical spline and 11.59 and 13.21 dB for the diagonal spline. These differences respect to corrugated horn are explained mainly by the shift in the beam waist and the PCL values (see Tables III and IV). From Fig. 6, we can see that the diagonal-spline horn provides a value closer to the desire 12.02 dB. The illumination efficiency loss due to this edge taper variation has been estimated to be lower than 1%, according to [19]. This is sufficiently good for testing a receiver band aimed to fully cover the ALMA Band-6 frequency range.

Based on our far-field radiation pattern simulations, it is possible to conclude that both horns have similar performance. However, based on our quasi-optical calculation, it can be seen that coupling of the diagonal-spline horn with the cold optical system of the Band-6 gives a higher illumination efficiency.
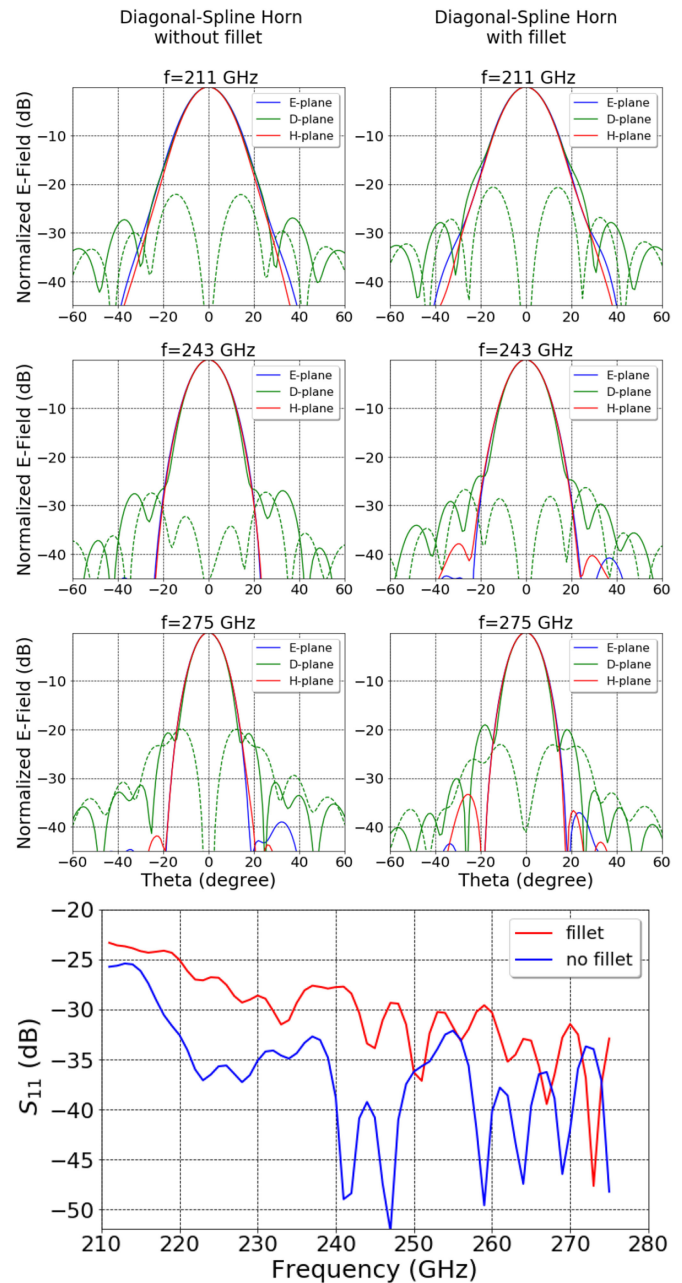
Fig. 7. (Top) Simulated far-field radiation pattern for the diagonal-spline horn with and without fillet. When the fillet is included the main difference is on cross polar (dashed line), which suffers a small degradation at 211 and 243 GHz but improves at 275 GHz. (Bottom) Return loss comparison. Small differences are visible, but performance is till < -23 dB over the entire frequency range.

With this point in mind, we selected the diagonal design for the fabrication and characterization. Furthermore, this design is easier to be fabricated in our workshop and does not require a complicated transition for connection with a rectangular wave-guide. In closing this section, it has to be remarked that the conical-spline horn design could be reoptimized to have better illumination efficiency. This could be achieved by including the PCL as an optimization goal in our HFSS model. Another option is to redesign the pair of elliptical mirrors to compensate the PCL shift. However, doing so is out of the scope of this article.
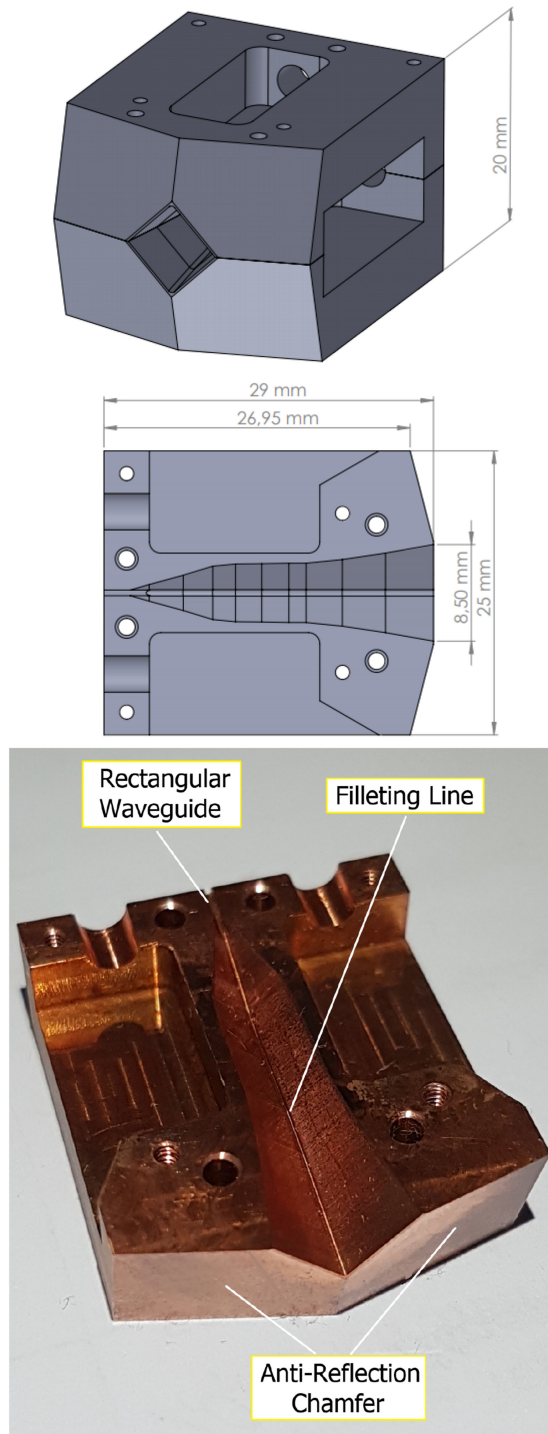
Fig. 8. (Top) Final design of the horn using the split-block technique. An antireflection chamfer of $30°$ was implemented to suppress the standing waves. (Bottom) One of the split blocks of the constructed horn. Construction took place at the Millimeter Wave Lab of the Universidad de Chile.

IV. CONSTRUCTION

The diagonal-spline horn was constructed using a high-precision computer numerical control milling machine in the split block configuration. The use of this technique results in an unavoidable filleting on the intersection line of two walls at the bottom of each block. The radius of the fillet equals
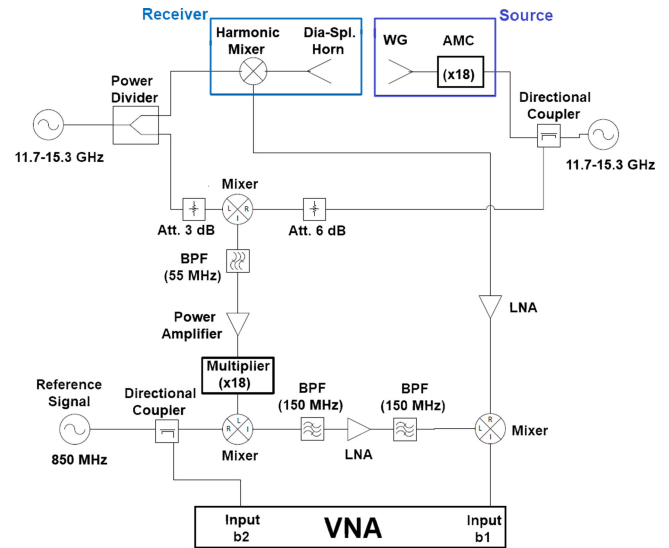

Fig. 9. Schematic of the receiver system used to characterize the horn. The receiver is formed by the diagonal-spline horn and a high-harmonic mixer. The RF source is formed by an open-ended waveguide connected to an active multiplication chain.
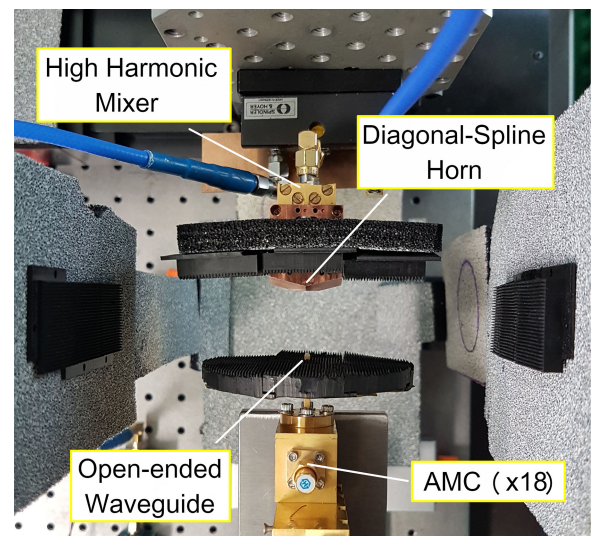
Fig. 10. Details of source–receiver setup used to measure the near-field radiation pattern. Only the last part of the active multiplication chain connected to the open-ended waveguide is shown in this picture.

that of the used mill, in this case, 0.3 mm. This fillet could be avoided if the broaching technique or five-axis machining with a square end mill were used to manufacture the horn. However, due to mechanical restrictions in our workshop, this technique was not implemented, but to evaluate the impact of this fillet, new simulations were carried out. Fig. 7 shows the latter simulations in comparison with the original ones. The main impact on the beam pattern lies on the D plane at 211 and 275 GHz. At 211 GHz, the cross polar gets a small degradation, but it is still under -20 dB, and the copolar component only starts making a visible difference at a level of -17 dB. At 275 GHz, the cross-polar component is reduced in around 3 dB, which represents significant improvement. The return loss shows the

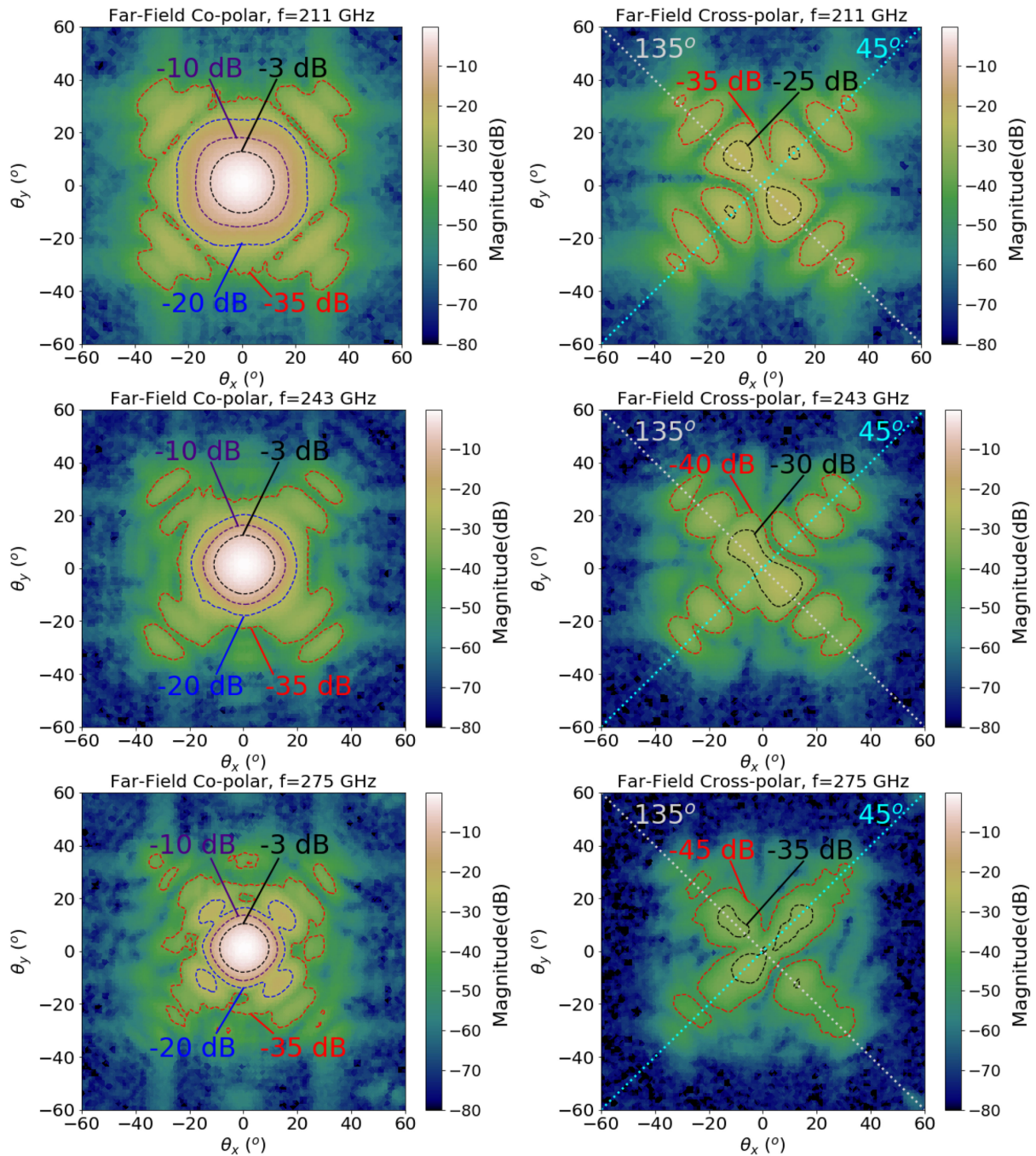Fig. 11. Measured copolar (left column) and cross-polar (right column) patterns at (top) 211 GHz, (middle) 243 GHz, and (bottom) 275 GHz. Contour lines for copolar measurements show the levels at -3, -10, -20, and -35 dB. For cross-polar measurements, a range of levels spanning from -25 to -45 dB are shown. Additionally, the cross-polar plots show the $45°$ and $135°$ planes using cyan and gray color lines, respectively.

same tendency, i.e., it degrades at low frequencies, but even at its highest point, the value remains below -23 dB. We, therefore, concluded that the necessary modifications that make the design feasible for machining, do not introduce disruptive changes in the overall horn performance.

The constructed horn is shown in Fig. 8. It uses flange based on specification UG-387 with tighter tolerances. This selection was made to facilitate its integration with commercial RF components. An antireflection chamfer of $30°$ was implemented in

the block in order to reflect the stationary waves out of the optical axis. Additionally, the block includes a waveguide interface in order to facilitate the integration to the external circuitry, making the block a few millimeter longer.

V. EXPERIMENTAL SETUP AND RESULTS

The characterization of the far-field radiation pattern can be achieved in two steps, measuring the near-field radiation
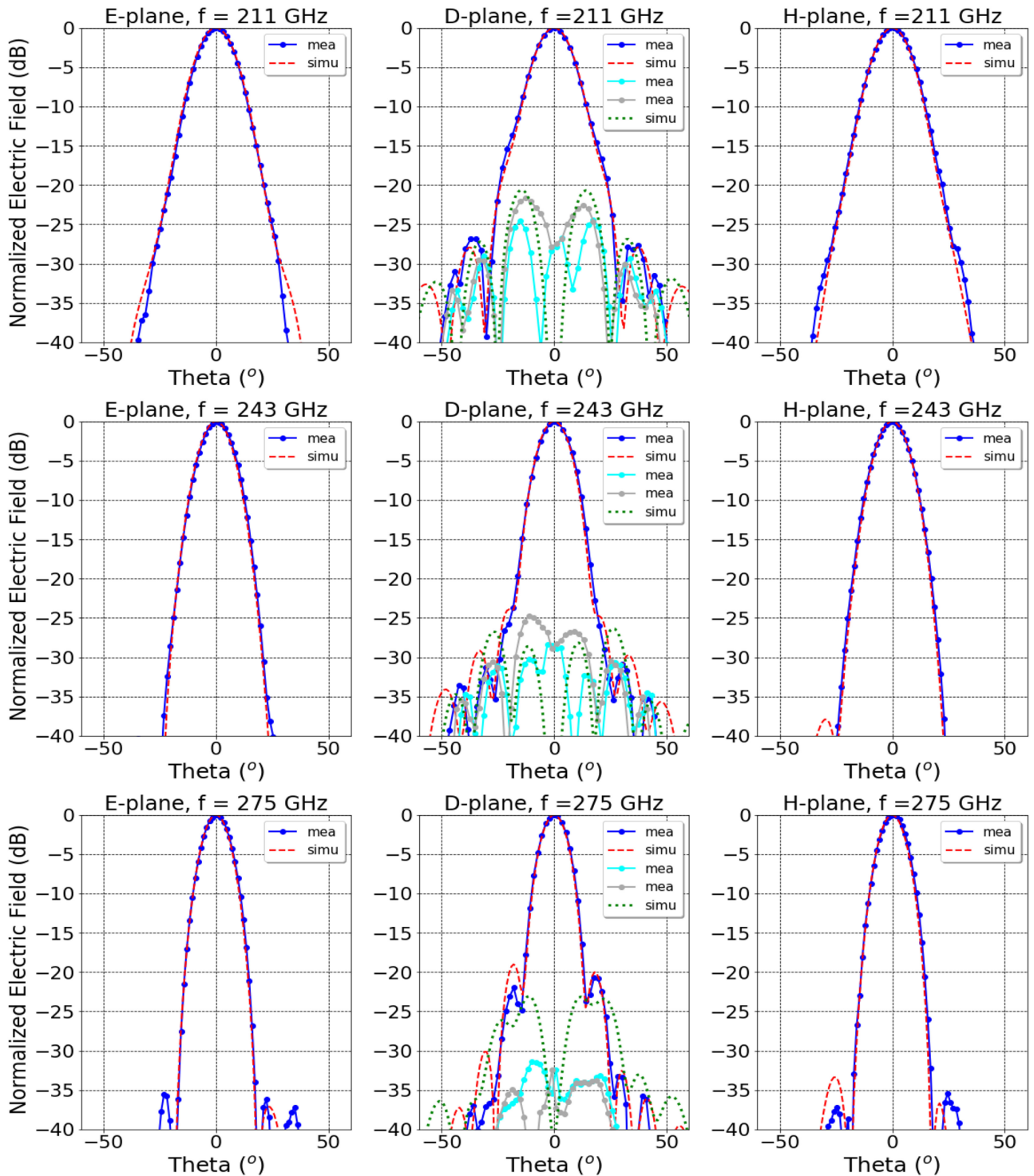
Fig. 12.   Comparison between experimental results (dotted lines) and simulations (dashed lines) for the far-field radiation pattern. Copolar comparison was made taking the cross section along the E and H planes (left and right column respectively), whereas cross-polar comparison (middle column) was made taking two cross sections at $45°$(cyan) and $135°$(gray), as shown in Fig. 11, using the same colors to facilitate the visualization.

pattern, and subsequently, using the Fourier transformation to obtain the desired far-field radiation pattern [23]. To obtain the far-field radiation pattern with this method, the amplitude and phase have been measured in the scanning plane, as described in [24]. This can be done by scanning the relative position between the RF source and the receiver. We have built our

own heterodyne receiver system, to operate at room temperature, using the technique described in [25]. The operation principle is as follows, the beam phase can be measured as long as there is a common phase reference between the RF signal and the local oscillator (LO) signal. The RF signal is radiated by the system source, whereas the LO signal is

used by the receiver to generate an intermediate-frequency (IF) signal.

Fig. 9 shows the block diagram of the circuitry used to build the receiver system. The ALMA Band-6 frequency range can be fully covered using signals generated between 11.7 and 15.3 GHz, in combination with a multiplication chain with a factor $N = 18$ (using one doubler and two triplers). Two signal generators are used to generate the RF and LO signal in this frequency range. The generated signals are divided using one directional coupler and one power divider. The idea is to mix the initial signals to obtain $f_1 - f_2 = \Delta f = 55.56$ MHz. Then, the down-converted signal is multiplied by a factor $N = 18$, obtaining a signal $f_3 = \Delta f \times 18 = 1000$ MHz. Once multiplied, the signal f_3 is mixed with a reference signal of frequency $f_{\text{ref}} = 850$ MHz. This provides an IF signal of 150 MHz, selected simply because of the available filters. The new IF undergoes a final mixing process, using as a second input the down-converted signal coming from the receiver system. Since we took a factor of $N = 18$ for down converting the RF signal coming from the source, the IF signal provided by the high-harmonic mixer has a frequency equal to f_3. The resulting output is a signal f_{out} whose frequency is equal to f_{ref}. Finally, the phase of the radiation pattern is obtained using a vector network analyzer to measure the ratio between f_{out} and f_{ref}.

Fig. 10 shows the near-field measuring setup. The diagonal-spline horn is directly connected to a high-harmonic mixer, making up the receiver system. An open-ended WR-4.3 waveguide is connected to an active multiplication chain, with a factor $N = 18$, used as an RF source. A microwave absorber has been used to eliminate the standing waves. Only the regions around radiating zones have been covered. Based on our experimental results we deem that this is a good alternative to a full implementation of an anechoic chamber. Copolar measurements were taken by aligning the receiver and source polarizations, and then, seeking for the peak power level, whereas for taking cross-polar measurements, the receiver system was rotated in $90°$ and the minimum power level was sought.

Fig. 11 shows the far-field experimental results for co and cross-polar at the key analysis frequencies. The transformation from near to far field was made by implementation of a script in *Python*. The signal-to-noise level is estimated to be around 65 dB. Fig. 12 shows a comparison of the far-field radiation patterns between experimental results and simulation. The plots show an excellent agreement for the copolar component at all the frequencies in the E, D, and H planes. Some small differences are observed only below -30 dB, making them almost negligible. The situation is different for the cross-polar component since more appreciable differences are visible. We have taken two profiles for cross-polar plots at $45°$ and $135°$ (green dotted lines at D-plane plots). Those profiles show unbalanced levels. The main explanation for this effect is the asymmetry between the two blocks of the horn. However, the cross-polar levels are, in most cases, lower than the theoretical prediction. Only at 243 GHz, the cross polar is higher than the simulated, but the peak value is still below -25 dB, which is certainly a very good result. Additionally, this horn presents sidelobe levels below -40 dB for the E and H planes, and levels below -20 dB for the D plane.

VI. CONCLUSION

We have designed two smooth-walled spline-profile horns, conical and diagonal. Simulations demonstrate that they have similar performance but we fabricated and characterized the latter since it adapts better to the design specifications. The measured radiation patterns have shown an excellent agreement with simulations. This horn has very good performance with a Gaussicity exceeding 96% and a cross-polar level lower than -20 dB over the entire frequency range. Additionally, we have demonstrated that it can be coupled to the astronomical systems by selecting the current ALMA Band 6 as an example. In this case, it would illuminate the subreflector with an efficiency loss lower than 1%.

The horn presented in this article is one of the first applications of the work presented by Gibson *et al.* [8], and certainly, the first at this specific frequency range. However, with the modifications presented here, our horn has a better performance since it can reach cross-polar levels as low as -30 dB for its higher design frequency. Moreover, the beam shape is clearly more circular is our design and has a larger fractional bandwidth of 26.3% (Gibson's design achieved only 17.5%).

The difficulty level to machining this horn can be classified as medium, i.e., easier than a corrugated, but harder than a classic conical or diagonal. This ease in machining along with the reduced tolerance restrictions, allow reducing the cost and production time of this sort of antennas. Additionally, this type of horn shows big integrability to the external circuitry since it can be constructed in a block along with a waveguide.

Finally, we believe that an easier construction process, ease in terms of integrability, high Gaussicity, and low level of cross polar, make this horn a good choice for millimeter and sub-millimeter receivers, especially when implementing focal plane arrays.

REFERENCES

[1] J. F. Johansson, "A comparison of some feed types," in *Multi-Feed Systems for Radio Telescopes* (Astronomical Society of the Pacific Conference Series), D. T. Emerson and J. M. Payne, Eds., vol. 75, Jan. 1995, pp. 82–89. [Online], Available: https://ui.adsabs.harvard.edu/abs/1995ASPC...75...82J

[2] A. Ludwig, "The definition of cross polarization," *IEEE Trans. Antennas Propag.*, vol. AP-21, no. 1, pp. 116–119, Jan. 1973.

[3] E. Muehldorf, "The phase center of horn antennas," *IEEE Trans. Antennas Propag.*, vol. AP-18, no. 6, pp. 753–760, Nov. 1970.

[4] A. Love, "The diagonal horn antenna," *Microw. J.*, vol. 5, pp. 117–112, 1962. [Online]. Available: https://www.microwavejournal.com/

[5] J. F. Johansson and N. D. Whyborn, "The diagonal horn as a sub-millimeter wave antenna," *IEEE Trans. Microw. Theory Tech.*, vol. 40, no. 5, pp. 795–800, May 1992.

[6] C. Granet, G. L. James, R. Bolton, and G. Moorey, "A smooth-walled spline-profile horn as an alternative to the corrugated horn for wide band millimeter-wave applications," *IEEE Trans. Antennas Propag.*, vol. 52, no. 3, pp. 848–854, Mar. 2004.

[7] G. James, "The feed system," *J. Elect. Electron. Eng.*, vol. 12, no. 2, pp. 137–145, 1992, doi:10.1109/MWSYM.1992.188258.

[8] H. J. Gibson *et al.*, "A novel spline-profile diagonal horn suitable for integration into THz split-block components," *IEEE Trans. THz Sci. Technol.*, vol. 7, no. 6, pp. 657–663, Nov. 2017.

[9] G. M. Rebeiz, L. P. B. Katehi, W. Y. Ali-Ahmad, G. V. Eleftheriades, and C. C. Ling, "Integrated horn antennas for millimeter-wave applications," *IEEE Antennas Propag. Mag.*, vol. 34, no. 1, pp. 7–16, Feb. 1992.

[10] G. Yassin *et al.*, "A high performance horn for large format focal plane arrays," in *Proc. 18th Int. Symp. Space THz Technol.*, 2007, p. 199. [Online]. Available: https://www.nrao.edu/meetings/isstt/papers/2007/2007199210.pdf .

[11] J. Leech, B. K. Tan, G. Yassin, P. Kittara, and S. Wangsuya, "Experimental investigation of a low-cost, high performance focal-plane horn array," *IEEE Trans. THz Sci. Technol.*, vol. 2, no. 1, pp. 61–70, Jan. 2012.

[12] V. Vilnrotter, M. Britcliffe, and D. Hoppe, "Focal plane array receiver for deep-space communication," in *Proc. IEEE Aerosp. Conf.*, Mar. 2008, pp. 1–10, doi:10.1109/AERO.2008.4 526 309.

[13] ALMA Partnership *et al.*, "The 2014 ALMA long baseline campaign: First results from high angular resolution observations toward the HL Tau region," *Astrophys. J. Lett.*, vol. 808, p. L3, Jul. 2015, doi:10.1088/2041-8205/808/1/L3.

[14] Event Horizon Telescope Collaboration *et al.*, "First M87 event horizon telescope results. VI. The shadow and mass of the central black hole," *Astrophys. J. Lett.*, vol. 875, p. L6, Apr. 2019, doi:10.3847/2041-8213/ab1141.

[15] B. N. Ellison *et al.*, "Corrugated feedhorns at terahertz frequencies - preliminary results," in *Proc. 5th Int. Symp. Space THz Technol.*, May 1994, pp. 851–860. [Online]. Available: https://ui.adsabs.harvard.edu/abs/1994stt..conf..851E

[16] C. Granet, G. James, R. Bolton, and G. Moorey, "Smooth-walled spline-profile horn for radio astronomy," in *Proc. JINA Int. Symp. Antennas*, 2002, vol. 1, pp. 375–378.

[17] *HFSS Ansoft*, ver. 19.1.0, Ansoft Corp., Pittsburgh, PA, USA, 2018. [Online]. Available: https://www.ansys.com/products/electronics/ansys-hfss

[18] J. Lamb *et al.*, "ALMA receiver optics design," ALMA Memo 362, 2001. [Online]. Available: http://library.nrao.edu/public/memos/alma/main/memo362.pdf

[19] P. F. Goldsmith and IEEE Microwave Theory and Techniques Society, *Quasioptical Systems: Gaussian Beam Quasioptical Propagation and Applications*. Piscataway, NJ, USA: Wiley-IEEE Press, 1998. [Online]. Available: https://ieeexplore.ieee.org/servlet/opac?bknumber=5264471

[20] A. Hammar, Y. Karandikar, P. Forsberg, A. Emrich, and J. Stake, "A 340 GHz high Gaussicity smooth spline horn antenna for the STEAMR instrument," in *Proc. IEEE Antennas Propag. Soc. Int. Symp.*, Jul. 2014, pp. 649–650, doi:10.1109/APS.2014.6 904 655.

[21] B. E. A. Saleh and M. C. Teich, *Fundamentals of Photonics*, 2nd ed. New York, NY, USA: Wiley-Interscience, 1991. [Online]. Available: https://trove.nla.gov.au/version/20427283

[22] A. Baryshev, M. Carter, W. Jellema, and R. Hesper, "Design and evaluation of ALMA band 9 quasioptical system," in *5th International Conference on Space Optics* (ESA Special Publication), B. Warmbein, Ed., vol. 554. Noordwijk, Netherlands: ESA Publications Division, Jun. 2004, pp. 365–371. [Online]. Available: https://ui.adsabs.harvard.edu/abs/2004ESASP.554..365B

[23] A. Yaghjian, "An overview of near-field antenna measurements," *IEEE Trans. Antennas Propag.*, vol. AP-34, no. 1, pp. 30–45, Jan. 1986.

[24] Y. Fujii *et al.*, "The first six ALMA Band 10 receivers," *IEEE Trans. THz Sci. Technol.*, vol. 3, no. 1, pp. 39–49, Jan. 2013.

[25] A. Gonzalez, Y. Fujii, T. Kojima, and S. Asayama, "Reconfigurable near-field beam pattern measurement system from 0.03 to 1.6 THz," *IEEE Trans. THz Sci. Technol.*, vol. 6, no. 2, pp. 300–305, Mar. 2016.

Rocio Molina received the B.Sc. and M.Sc. degrees in electrical engineering from the Universidad de Chile, Santiago, Chile, in 2015 and 2017, respectively. Her M.Sc. thesis topic was the design of optics for heterodyne cameras in millimeter waves.

Since 2014, she has been an Active Member with the Millimeter Wave Laboratory, Astronomy Department, University of Chile, where she has been mainly involved with the design of antennas and other optical devices, including the optics for heterodyne cameras in millimeter waves.

Andrey Khudchenko received the M.S. degree in applied physics and mathematics and the Ph.D. degree in radiophysics from the Moscow Institute of Physics and Technology, Moscow, Russia, in 2007 and 2009, respectively.

From 2004 to 2008, he was an Engineer, and in 2009, a Researcher with the Kotel'nikov Institute of Radio Engineering and Electronics, Russian Academy of Sciences, Moscow. Since 2009, he has been an Instrument Scientist with The Netherlands Institute for Space Research SRON, Groningen, The Netherlands. It includes development of sideband-separating receiver for the ALMA band 9, CHAMP+ high mixers for the APEX telescope, and work on the stabilization of quantum cascade lasers for hot electron bolometer receivers.

Ronald Hesper received the M.Sc. degree in experimental solid state physics from the University of Leiden, Leiden, The Netherlands, in 1994 and the Ph.D. degree in experimental solid state physics from the University of Groningen, Groningen, The Netherlands, in 2000.

Since 2000, he has been an Instrument Scientist with the Kapteyn Astronomical Institute, University of Groningen. From 2000 to 2008, he was involved in the technological development of the ALMA Band 9 receivers, including the process of industrialization, as well as related projects like the CHAMP+ mixer arrays for APEX; from 2008 to 2013, on the development of a sideband-separating mixer upgrade for the ALMA Band 9 receivers; and from 2013 to the beginning of 2015, on the industrialization of the ALMA Band 5 receivers. He is currently involved in the development of new (arrayable) heterodyne detector technologies at frequencies around 1 THz.

Daniel Arturo Montofré received the B.Sc. degree in physics engineering from the Universidad Chile, Santiago, Chile, in 2014. He is currently working toward the double Ph.D. degree in electrical engineering and astronomy with the Universidad de Chile, Santiago, Chile, and the University of Groningen, Groningen, The Netherlands, respectively.

His research interests include the development of horn antennas for millimeter/submillimeter astronomical instrumentation, design of frequency selective filters, and quasi-optical design for dual-band observations.

Andrey M. Baryshev received the master's degree (summa cum laude) in physical quantum electronics from the Moscow Institute of Physics and Technology, Moscow, Russia, in 1993, and the Ph.D. degree in superconducting integrated receiver from the Technical University of Delft, Delft, The Netherlands, in 2005.

He is currently a Senior Instrument Scientist with the University of Groningen, The Netherlands. Since 1998, he has been with the SRON Low Energy Astrophysics Division and the Kapteyn Astronomical Institute, University of Groningen, Groningen, The Netherlands. Since 2000, he has been involved in a joint effort to develop the SIS receiver (600–720 GHz) for ALMA. In 2013, he became an Associate Professor of astronomical instrumentation for the far-infrared with the Kapteyn Astronomical Institute, University of Groningen. His main research interests include the areas of heterodyne and direct detectors for large focal plane arrays at terahertz frequencies, and quasi-optical system design and experimental verification.

Dr. Baryshev was the recipient of the Netherlands Organisation for Scientific Research-VENI grant for research on heterodyne focal plane array technology in 2008, and an EU commission Starting Researcher Grant for work on direct detector focal plane arrays in 2009.
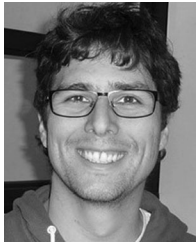
Nicolas Reyes received the Ph.D. degree in electrical engineering from the Universidad de Chile, Santiago, Chile, in 2013.

In 2013, he joined the Max Planck Institute for Radio Astronomy, Bonn, Germany, as a Postdoctoral Researcher for the SOFIA Project, where he was involved in terahertz instrumentation and multipixel receivers. In 2015, he was with the Millimeter/Submillimeter Wave Laboratory, Universidad de Chile. He is currently an Assistant Professor with the Electrical Engineering Department, Universidad de Chile. His current research interests include low-noise electronic, antennas, numerical simulation, and radio astronomy instrumentation.

Fausto Patricio Mena received the B.S. degree in physics from the Escuela Politcnica Nacional, Quito, Ecuador, in 1994, and the M.S. and Ph.D. degrees in physics from the University of Groningen, Groningen, The Netherlands, in 2000 and 2004, respectively.

He is currently an Associate Professor with the Electrical Engineering Department, Universidad de Chile, Santiago, Chile. In 2004, he joined the Netherlands Institute for Space Research, Groningen, as an Instrument Scientist with the Low Energy Division. In 2008, he moved to the Universidad de Chile, where he cofounded the Radio Astronomical Instrumentation Group and the Millimeter Wave Laboratory.